



The case for increasing the posting rate in delay/Doppler altimeters

Alejandro Egido^{a,b,*}, Salvatore Dinardo^c, Christopher Ray^{a,d}

^aNOAA Laboratory for Satellite Altimetry, 20740 College Park, MD, USA

^bGlobal Science & Technology, Inc., 20770 Greenbelt, MD, USA

^cHeSpacELUMETSAT, 64295 Darmstadt, Germany

^dSaint Mary's College of California, 94575 Moraga, CA, USA

Received 3 July 2019; received in revised form 7 March 2020; accepted 11 March 2020

Available online 31 March 2020

Abstract

In this paper we analyze the effect of increasing the posting rate of delay/Doppler altimeters on the retrieval of open ocean geophysical parameters. The conventional posting rate for synthetic aperture radar altimeters data is 20 Hz, which on-ground corresponds to the typical delay/Doppler along-track resolution of about 320 m. However, the speckle autocorrelation properties of delay/Doppler waveforms over the open ocean show a decorrelation distance much shorter than the typical along-track resolution, suggesting that further information can be extracted if more frequent observations of the surface were obtained. By processing one cycle of Sentinel-3A data at different posting rates we have verified that a relative improvement of more than 20% in the measurement noise of both sea surface height and significant wave height can be achieved, just by increasing the posting rate from 20 to 40 Hz, and an even further improvement is obtained at 80 Hz. We believe this result has significant implications for the current CryoSat-2 and Sentinel-3 missions and the upcoming Sentinel-6/Jason-CS mission.

© 2020 Published by Elsevier Ltd on behalf of COSPAR.

Keywords: Delay/Doppler altimetry; Sentinel-3; Sea surface height; Significant wave height

1. Introduction

Since its conception, satellite altimetry has been a major breakthrough in the field of ocean surface topography, allowing scientist to significantly improve their understanding of ocean processes at global scales. From Geos-3 in 1975, through the TOPEX/Poseidon Mission launched in 1992, to the Jason altimeter series, including Jason-1 in 2001, Jason-2 in 2008 and ultimately Jason-3 in 2016 (the current reference mission of the Ocean Surface Topography satellite series) satellite radar altimeters have used the same data processing scheme. Referred to as

“conventional” or low resolution mode (LRM), this technique is based on the continuous transmission of radar pulses, which are then power detected and incoherently averaged. This process, also known as multilooking, reduces the measurement uncertainty and enables the reliable estimation of geophysical parameters.

The introduction of the delay/Doppler (D/D) altimetry concept (Raney, 1998), posed a new paradigm in the field of radar altimetry. In this technique a fast Fourier transform (FFT) is applied to a set of pulses transmitted in bursts to separate the contributions of the scatterers within the antenna beamwidth into Doppler frequency bins. The FFT operation on the complex echoes performs in essence an unfocused synthetic aperture radar (SAR) calculation, which reduces the altimeter footprint along the flight direction by an order of magnitude with respect to LRM

* Corresponding author at: NOAA Laboratory for Satellite Altimetry, 20740 College Park, MD, USA.

E-mail address: alejandro.egido@noaa.gov (A. Egido).

altimeters. The range migration of the scatterers within the antenna footprint is corrected by an unambiguous relationship with frequency. The Doppler bins from successive bursts illuminating coincident locations on the surface are then accumulated to obtain the final multilooked (D/D) waveform. Through this process, in addition to an improved along-track resolution, the D/D altimeter achieves a significant improvement in effective number of looks (ENL), which can be regarded as the number of independent observations obtained by the radar from a distributed target per unit of time, and leads to a noise reduction in the estimation of geophysical parameters (Wingham et al., 2006; Raney, 2012).

In April 2010, the European Space Agency (ESA) launched Cryosat-2, the first satellite radar altimeter to incorporate SAR mode capability. Initially devoted for cryosphere sciences, the Synthetic Aperture Interferometric Radar Altimeter (SIRAL) on-board CryoSat has also provided the opportunity to demonstrate and study the performance of the D/D altimetry technique over the ocean (Phalippou and Demestere, 2011). Later on, in February 2016, ESA launched the Sentinel-3A mission, incorporating a SAR altimeter similar to SIRAL, and finally, in April 2018 the constellation was completed with a companion satellite, Sentinel-3B. LRM altimeters have been designed aiming for consecutive echoes to be essentially decorrelated from each other. This allows to make the satellite operation efficient in terms of power usage while maximizing the information obtained from the transmitted radar pulses. Following these criteria, the pulse repetition frequency (PRF) for the Jason altimeter series was selected to be approximately 2 kHz (Walsh, 1982; Rodriguez and Martin, 1994). A later study showed using CryoSat-2 data in a pseudo-low resolution mode (PLRM) fashion (Egido and Smith, 2019), that 2 kHz is a conservative upper limit for the PRF, and that it is possible to improve the estimation of geophysical parameters transmitting pulses at higher PRFs. In this study we follow a similar rationale as in the previously cited paper, but concentrating on the delay/Doppler altimeter.

The D/D algorithm implemented in CryoSat-2 and Sentinel-3, applies coherent processing to the 64 echoes within each burst (equivalent to 3.5 ms of flight) through an along-track fast Fourier transform (FFT). Taking into account that pulses are transmitted at a PRF of approximately 18 kHz, the 64 resulting Doppler bins have a bandwidth of about 280 Hz, which projected on the surface lead to a resolution of about 320 m in the along-track direction. The typical posting rate for D/D is 20 Hz, corresponding also to the along-track resolution, and thus ensuring minimum overlap between footprints of adjacent waveforms. However, this is also a conservative value for the D/D posting rate. In previous studies (Dinardo et al., 2015), it was shown how by increasing the posting rate from 20 Hz to 80 Hz it was possible to reduce the noise in the estimation of geophysical parameters. In this paper we consolidate and expand that result and provide a physical

justification based on the correlation properties of the multilooked SAR waveforms.

2. Data processing methodology

For this study we used the National Oceanic and Atmospheric Administration (NOAA) Laboratory for Satellite Altimetry (LSA) Experimental SAR Processor. This is an in-house developed software, that allows for the computation of fully-focused SAR (FF-SAR) (Egido and Smith, 2017), D/D and PLRM data. The code has the capability to process both Sentinel-3 and CryoSat-2 data, from Level-1A or Full-Bit Rate (FBR) data (uncalibrated single complex echoes) to Level-2 or geophysical parameters.

Multiple processing options can be configured in the processor. Apart from the fully-focused or delay/Doppler processing, configurable options include: zero-padding of selectable size; different windowing options in the across-track and along-track dimension; configurable aperture length; configurable focal point selection (zero-Doppler or nadir); different multilooking options; and antenna pattern compensation.

The D/D waveforms are obtained in the NOAA/LSA Processor as a by-product of the FF-SAR processing. It can be shown, although it is out of the scope of this paper, that applying a coherent summation burst-by-burst to the range migrated and phase compensated echoes, as described in Egido and Smith (2017), results in the D/D stack. This process is equivalent to applying the exact beam-rocking, along-track beam-forming, and later stacking, as it would be performed in a precise D/D processing calculation (Wingham et al., 2006).

The most significant difference between these two methods is that in the FF-SAR processing approach presented in Egido and Smith (2017) a back-projection algorithm is used, where the range cell migration correction (RCMC) is performed accounting for the geometrical range variation with respect to a focal point of every single echo in the aperture. On the contrary, in standard D/D processing (Raney, 1998), the RCMC is applied as a function of Doppler frequency, which implies that a single RCMC value is applied to each burst, usually with respect to the central position of the Doppler beam, thus incurring in a small error in the RCMC for the first and last echoes in the burst. This effect has been described as “range-walk” (Guccione, 2008), and suitable mitigation strategies have already been presented to correct for it (Scagliola et al., 2021).

For our analysis we have processed one full cycle of Sentinel-3A data over the open ocean with the standard processing options: zero-padding by a factor of two in range, no windowing in either dimension, and no antenna pattern compensation. The estimation of geophysical parameters, i.e. sea surface height (SSH), significant wave height (SWH), and radar-backscatter (σ^0), is performed by means of waveform retracking process, in which the SAMOSA model (Ray et al., 2015), is fitted to the D/D

waveforms by means of a Levenberg-Marquardt least mean squares error minimization algorithm.

We consider in this study the effect of increasing the posting rate of the D/D processing on the final estimation of geophysical parameters. For that, we compute the D/D waveforms at a posting rate of 20, 40 and 80 Hz. For the 40 Hz and 80 Hz posting rates, we perform the retracking directly on the 40 or 80 Hz waveforms and average the results to 20 Hz, as opposed to multilooking the high posting rate waveforms first down to 20 Hz. While both methods should, in theory, provide similar results, in practice, retracking the 20 Hz multilooked waveforms is a much more problematic operation. To multilook the high posting rate waveforms to 20 Hz it is first necessary to realign the waveforms to a common reference range. In rough sea state conditions, when the SSH noise is much higher the location of the waveform's leading edge is less stable, and therefore the multilooking process smears the leading edge. Although not shown in this paper, we verified that by retracking the 20 Hz multilooked waveforms significant biases are introduced in the estimation of SWH, particularly towards rougher sea state condition. For this reason we opted for retracking the 80 Hz waveforms and later averaging.

In the following section we discuss the correlation properties of the speckle pattern in D/D waveforms, which ultimately limits the amount of independent observations that may be obtained of the ocean surface.

3. Delay/Doppler waveforms speckle autocorrelation and effective number of looks

As in most radar remote sensing systems, speckle governs the signal properties of altimeters echoes scattered off the ocean surface. Although generally referred to as “speckle noise”, speckle is actually inherent to the scattering process of radar pulses off a rough surface such as the open ocean. In this context, the great dispersion in signal power (the power distribution of the individual radar echoes can be described as a decaying exponential function) makes the use of individual waveforms virtually intractable. In order to mitigate the effect of speckle, a “multilooking” process is required, i.e., the incoherent combination of power detected echoes recorded from nearby locations on the surface. In D/D altimetry, each Doppler beam obtained after the along-track FFT constitutes a random realization of the speckle scattering process. In this case, multilooking is achieved by incoherently averaging the beams from successive bursts pointing to the same along-track location.

The speckle correlation properties determine the statistical independence of consecutive observations of the surface, and consequently limit the maximum achievable ENL. As shown in [Quarty et al. \(2001\)](#) and [Wingham et al. \(2006\)](#), the ENL can be computed as the ratio between the squared mean power of the radar echoes and

the power variance. The higher the ENL the more efficient the speckle noise mitigation, and therefore, the lower the error in the final estimation of geophysical parameters.

In this section, we analyze the speckle correlation properties by means of the autocorrelation function (ACF) of the multilooked D/D waveforms in the along-track dimension. This allows us to determine the decorrelation length, i.e. the minimum distance at which adjacent D/D observations can be considered to be uncorrelated. For that, we perform the D/D processing at a posting rate much higher than their native resolution. In this case, we set up the processor to compute a multilooked waveform every 7.5 meters along the satellite track.

For the computation of the multilooked D/D waveforms ACF we processed a Sentinel-3A track over the East Pacific Ocean with varying sea state conditions. After D/D processing, the waveform were range migrated to a common reference range based on the retracked sea surface height, forcing all the waveforms to be aligned at the same range gate within the sampling window. To obtain a precise estimation of the ACF, we computed the ACF of all waveforms within one given second and then average the ACFs over sections of about 400 km along the track with stable SWH and σ^0 conditions.

The results of the ACF are depicted in [Fig. 1](#). In [Fig. 1a](#) we show the ACF in gray color scale as a function of the waveform range gate and the correlation distance. The ACF is represented in dB scale for better visualization. In this case, we show the ACF for an SWH of 2 m and a standard deviation of 35 cm over 400 km along the track. As can be observed, except for the earlier range gates of the waveform corresponding to the thermal noise region, where the autocorrelation function is noticeably narrower, the ACF width is fairly constant throughout the rest of the waveform. This can be better seen in [Fig. 1b](#). The curves with different colors correspond to cuts at different range gates of the ACF, as indicated by the vertical dashed lines of matching color in [Fig. 1a](#). We observe that the ACF drops below $1/e$, where e is the Euler's number, (a standard measure beyond which signals are considered to be essentially uncorrelated) for an along-track distances as low as 160 m, which would suggest that more information may be obtained from the D/D waveforms at a higher posting rate than their typical along-track resolution. For completeness, we have also included in this figure the ACF cuts for a SWH of 4.5 m with a standard deviation of 50 cm, showing an increase in the decorrelation distance with sea state. This result was unexpected, and we shall come back to this issue in the Discussion section.

The fact that the decorrelation length is shorter than the native D/D along-track resolution has significant implications when considering the effective number of looks at different posting rates. In [Fig. 2](#) we show the 20 Hz ENL for the three different posting rates considered in this study for a SWH of 2 m. In order for the ENL to be comparable among them, both the 40 and 80 Hz waveforms are

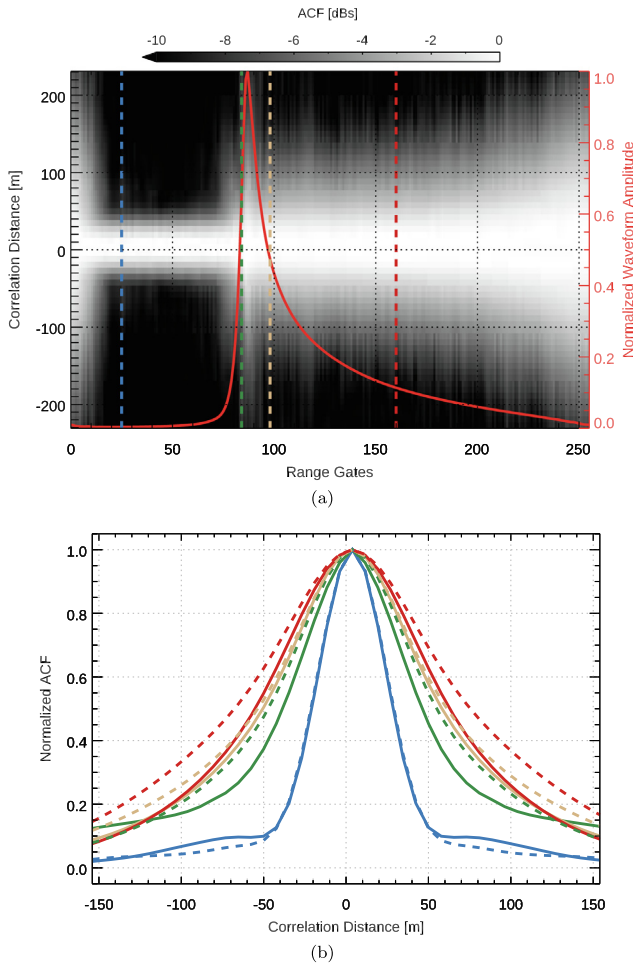


Fig. 1. Pulse-to-pulse autocorrelation, R , for CryoSat FBR SAR mode echoes for a relatively calm ocean, i.e. $SWH \approx 2$ m. (a) R as a function of both range gate, g , and pulse lag, k . R is represented in dB for a better visualization of the autocorrelation structure. The average waveform for the whole observation period is overlaid in a solid red curve. The vertical lines indicate R cuts along k for different range gates. (b) R cuts along k . The different colors correspond to cuts for different range gates, as indicated by vertical lines with matching color in (a). Solid lines correspond to $SWH \approx 2$ m, and dashed lines to $SWH \approx 4.5$ m.

multilooked down to 20 Hz. The 80 Hz posting rate observations present the highest ENL of the set throughout all range gates of the waveform. However, the biggest increase takes place when increasing the posting rate from 20 to 40 Hz. This is more evident when considering the ENL ratio. When increasing the posting rate from 20 to 40 Hz, we observe an average increase in the ENL by a factor of 1.8 throughout the whole waveform. This suggests that at a 40 Hz posting rate, corresponding to an along-track distance of about 160 m, adjacent delay/Doppler waveforms are essentially uncorrelated, in agreement with the decorrelation distance observed on Fig. 1b. For the 80 Hz posting rate, the average ENL increase factor is of 2.4. This increase is more moderate than in the previous case, but the results indicate that a higher noise reduction in the

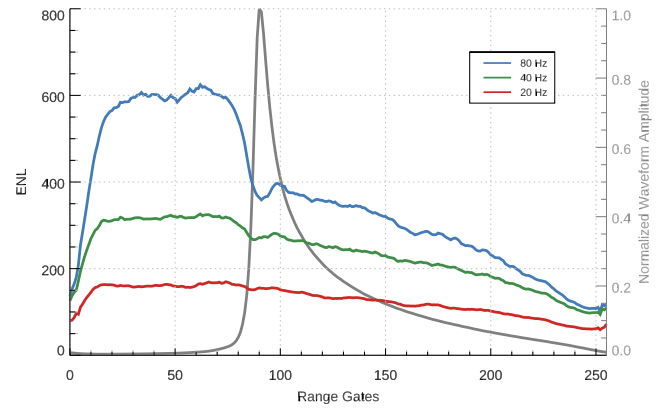


Fig. 2. Effective number of looks as a function of waveform range gate for a relatively calm ocean, i.e. $SWH \approx 2$ m, at different posting rates: 20 Hz, in red; 40 Hz in green; 80 Hz in blue. For reference, the gray line shows the average normalized power waveform period (50 s).

retrieval of geophysical parameters can be obtained by increasing the posting rate even further.

4. Performance analysis

To assess the performance of the D/D altimeter processing at different posting rates, we compute the geophysical parameters measurement noise as the standard deviation of the 20 Hz retrieved parameters around their 1 Hz mean value, i.e. the 20 Hz root mean square (RMS) noise. Those are then binned together according to their estimated SWH value to compute the data statistics as a function of sea state. Fig. 3 depicts the box-whisker plot for the geophysical parameters estimated by the retracker, i.e. SSH, SWH, and σ^0 . For completeness, the top panel in the figure shows the number of measurements per SWH bin. In the three other panels, we represent in different colors the RMS errors for the 20, 40 and 80 Hz posting rates.

The RMS noise for the 20 Hz posting rate shows the standard performance of the delay/Doppler method. These results are fully consistent with what was reported in previous studies, such as (Phalippou and Demestere, 2011; Scagliola et al., 2015). When the posting rate is increased to 40 Hz, the RMS noise values experience a significant drop throughout the whole sea state range considered in the analysis. An even further decrease in measurement noise is observed when the posting rate is increased to 80 Hz. The latter is, however, less significant than when going from 20 Hz to 40 Hz, as expected due to the estimated decorrelation distance and evolution of the ENL shown in the previous section.

For a more quantitative assessment of this performance improvement, we show in Fig. 4 the relative error of the geophysical parameters measurement noise estimated from the 40 and 80 Hz data, with respect to the standard 20 Hz RMS values. For all three parameters, the RMS noise

Table 1
Overall relative error improvement (in percentage) for the different geophysical parameters for the 40 and 80 Hz posting rates with respect to the 20 Hz data.

Parameters	40 vs 20 Hz	80 vs 20 Hz
SSH	21.0	23.6
SWH	22.0	25.8
Sig0	17.3	22.6

improvement peaks around 1 m SWH and decreases towards rougher sea state conditions. In addition, the RMS error shows a non-negligible improvement for the 80 Hz posting rate when compared to the 40 Hz one, particularly in low SWH conditions, where the RMS error improvement is higher than 25% for both SSH and SWH, for all SWH values below 2 m. In terms of measurement accuracy, we verified that the 80 Hz observations are essentially unbiased with respect to the 20 Hz ones, with no apparent sea state dependent trends.

We compute the overall relative error improvement for each parameter as the average RMS error for the whole

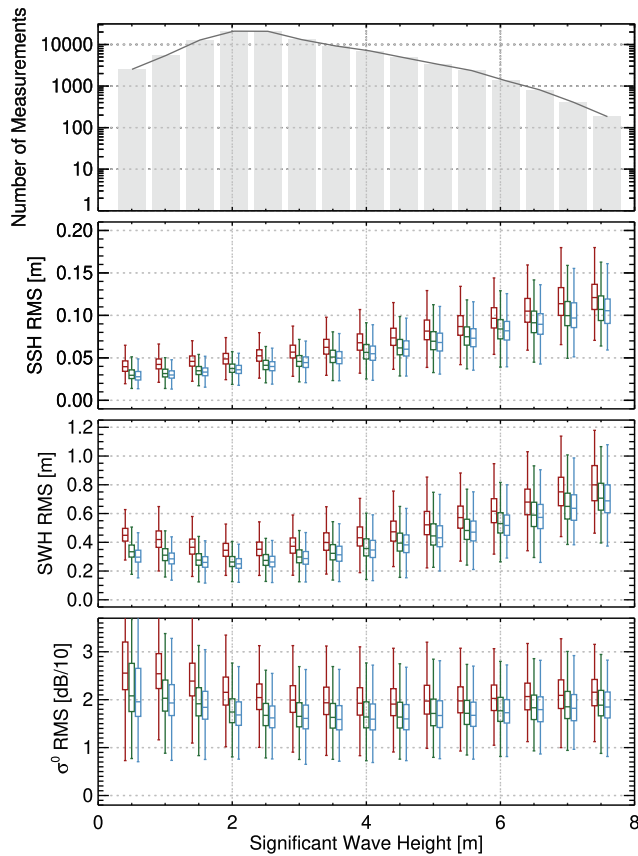


Fig. 3. Box-whisker plots of the retracked geophysical parameters 20 Hz RMS noise as a function of SWH. The boxes show the median, first and third quartile of the RMS per SWH bin, whereas the whiskers represent the 1.5 inter-quartile range with respect to the median. The different colors correspond to the three different posting rates: 20 Hz in red; 40 Hz in green; and 80 Hz in blue. The top panel shows the number of measurements per SWH bin.

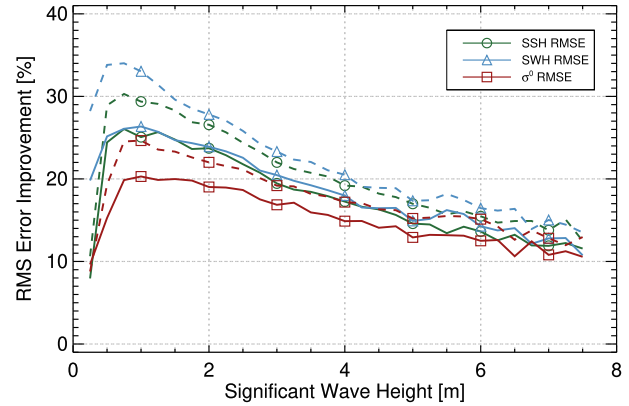


Fig. 4. Geophysical parameter estimation relative RMS noise improvement. In solid lines, relative RMS error improvement between the 20 Hz and 40 Hz posting rates. In dashed lines, relative RMS error improvement between the 20 Hz and 80 Hz posting rates.

SWH range. The results are gathered in Table 1. We observe that by increasing the posting rate to 40 Hz an improvement of more than 20% error reduction can be obtained for both SSH and SWH. In addition, and despite the fact that increasing the posting rate further to 80 Hz does only improve the RMS noise by about 4%, the improvement can be quite significant for calm sea states, as we have observed above.

5. Discussion

The reduction in the geophysical parameters measurement noise achieved by increasing the D/D waveforms posting rate to 40 or 80 Hz stems from the fact that the along-track decorrelation distance in the open ocean is much shorter than the on-ground distance between consecutive waveforms given by the typical 20 Hz posting rate that has typically been used for these data.

In a previous study (Egido and Smith, 2019), we found a similar effect for LRM and determined that increasing the PRF of LRM altimeters could lead to significant improvements in the estimation of geophysical parameters. A discrepancy that we have observed between both studies is that, as opposed to the LRM case, in D/D the relative RMS error improvement decreases with wave height, as can be observed in Fig. 4. This is linked to how the ENL evolves with sea state.

In LRM, without coherent processing in the along-track dimension, the LRM altimeter footprint is defined by the pulse-limited area, which can range between 1.5 and 7 km, depending on sea state conditions. The increase in the active scattering area leads to a shorter pulse-to-pulse decorrelation distance, and therefore higher ENL, which in turn contributes to a higher RMS error improvement.

In the D/D case, the ENL decreases with SWH. This observation had already been made in Scagliola et al. (2015). In Fig. 5 we reproduce these results together with

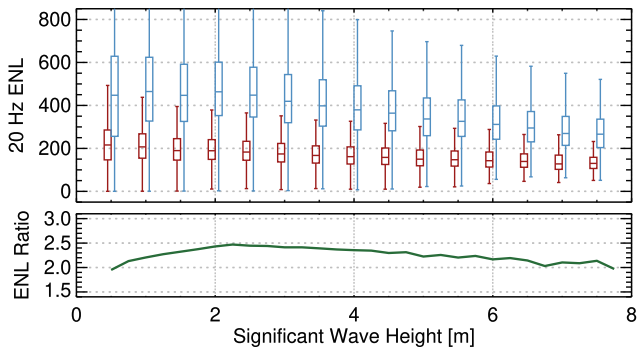


Fig. 5. (Top) ENL at the waveform tracking point as a function of SWH for the 20 Hz (red) and 80 Hz (blue) posting rates. (Bottom) ENL ratio for both the 20 Hz and 80 Hz posting rates.

the 80 Hz vs 20 Hz ENL ratio. The decrease in both the total ENL and the ENL ratio can be related to the fact that D/D waveforms become increasingly more correlated with each other as the sea state gets rougher. Indeed, as shown in Fig. 1c, the ACF curves show a significant widening for higher SWH. The root cause of this behavior is still under investigation.

The observed increase in decorrelation distance with SWH seems to be in contradiction with the findings from a previous study (Wingham et al., 2018), where the power correlation coefficient for the single D/D beams was computed as a function of along-track distance using a theoretical waveform model. In agreement with our observations, the authors obtained decorrelation lengths much shorter than the typical D/D along-track resolution, with decorrelation lengths increasing with look angle. In that study, however, the decorrelation length for the individual Doppler beams was predicted to decrease with SWH.

Although that is apparently a discrepancy with our findings, it should be noted that in this paper we compute the correlation of the D/D multilooked waveforms. The latter can be regarded as the weighted average of the single Doppler beam correlation functions, where the weights are the relative power of the individual Doppler beams. As the relative power of Doppler beams at higher look angles increases with SWH, the outer Doppler beams could end up dominating the multilooked waveform correlation, resulting in longer decorrelation distances at higher SWH values. This hypothesis will need to be further analyzed in future studies to clarify this potential discrepancy.

6. Conclusions

In this paper we have shown how increasing the posting rate of delay/Doppler altimeter observations can improve the estimation of geophysical parameters over the open ocean. Thanks to a narrower decorrelation length than it was previously thought, it is possible to increase the posting rate of D/D waveforms beyond the typical 20 Hz

(what corresponds on-ground to the D/D altimeter along-track resolution) to extract more information out of the SAR altimeter data.

When increasing the posting rate to 40 Hz, we observe an overall relative improvement in the SSH and SWH measurement noise of 21% and 22%, respectively, whereas for the radar back-scattering the improvement amounts to 17%. Using a posting rate of 80 Hz decreases further the measurement noise by about 4% in all parameters. The improvement is more significant for low SWH conditions and decreases gradually towards rougher sea states. For instance, at 80 Hz the error reduction for SSH and SWH is higher than 25% for all sea states below 2 m, and peaks over 30% for SWH values around 1 m.

In addition to the performance improvement in the open ocean, increasing the posting rate of the D/D data could also be beneficial for other altimetry applications in areas where the surface is more heterogeneous. Such is the case of the polar oceans, coastal zones, and in-land waters, where the higher posting rate could contribute to a better sampling of the surface.

As a final remark we note that, while performing the D/D processing at higher posting rates would necessarily imply an increase in the processing time and data volume of some science products, these issues become less important with the constantly growing computational power and storage capabilities. In addition, implementing this change in the processing would require minimal modifications in the SAR processors and data products. For instance, all Level-2 products could remain the same and just intermediate Level-1b products would need to be modified.

We believe the results presented in this paper are particularly relevant for current and future SAR altimetry missions, such as CryoSat-2, Sentinel-3 and Sentinel-6, and could constitute a straightforward approach to achieve a significant reduction in the measurement noise of the geophysical parameters obtained from SAR altimetry data.

Acknowledgements

The contents of this paper are solely the opinions of the authors and do not constitute a statement of policy, decision, or position on behalf of NOAA or the U.S. Government. This research was supported by the NOAA component of the NASA-NOAA Joint program announced in NASA Research Announcement (NRA) NNH16ZDA001N, Research Opportunities in Space and Earth Science (ROSES-2016), Program Element A.11: Ocean Surface Topography Science Team.

References

- Dinardo, S., Scharroo, R., Benveniste, J., 2015. SAR Altimetry at 80 Hz: Open Sea, Coastal Zone, Inland Water. Ocean Surface Topography Science Team Meeting.

- Egido, A., Smith, W.H.F., 2017. Fully FOCUSED SAR altimetry: theory and applications. *IEEE Trans. Geosci. Remote Sens.* 55, 392–406.
- Egido, A., Smith, W.H.F., 2019. Pulse-to-pulse correlation effects in high prf low-resolution mode altimeters. *IEEE Trans. Geosci. Remote Sens.* 57, 2610–2617.
- Guccione, P., 2008. Beam sharpening of delay/doppler altimeter data through chirp zeta transform. *IEEE Trans. Geosci. Remote Sens.* 46, 2517–2526.
- Phalippou, L., Demestere, F., 2011. Optimal re-tracking of sar altimeter echoes over open ocean: theory versus results for SIRAL2 data. In: 2011 OSTST Meeting, San Diego, CA, USA.
- Quarty, G.D., Srokosz, M.A., McMillan, A.C., 2001. Analyzing altimeter artifacts: statistical properties of ocean waveforms. *J. Atmosf. Oceanic Technol.* 18, 2074–2091.
- Raney, R.K., 1998. The delay/doppler radar altimeter. *IEEE Trans. Geosci. Remote Sens.* 36, 1578–1588.
- Raney, R.K., 2012. Cryosat sar-mode looks revisited. *IEEE Geosci. Remote Sens. Lett.* 9, 393–397.
- Ray, C., Martin-Puig, C., Clarizia, M.P., Ruffini, G., Dinardo, S., Gommenginger, C., Benveniste, J., 2015. Sar altimeter backscattered waveform model. *IEEE Trans. Geosci. Remote Sens.* 53, 911–919.
- Rodriguez, E., Martin, J.M., 1994. Correlation properties of ocean altimeter returns. *IEEE Trans. Geosci. Remote Sens.* 32, 553–561.
- Scagliola, M., Dinardo, S., Fornari, M., 2015. An extended analysis of along-track antenna pattern compensation for sar altimetry. In: *Proceedings of 2015 IEEE International Geoscience and Remote Sensing Symposium (IGARSS)*, pp. 1238–1241.
- Scagliola, M., Recchia, L., Maestri, L., Giudici, D., 2021. Evaluating the impact of range walk compensation in delay/doppler processing over open ocean. *Adv. Space Res.* 68, 937–946. <https://doi.org/10.1016/j.asr.2019.11.032>.
- Walsh, E.J., 1982. Pulse-to-pulse correlation in satellite radar altimeters. *Radio Sci.* 17, 786–800.
- Wingham, D., Francis, C., Baker, S., Bouzinac, C., Brockley, D., Cullen, R., de Chateau-Thierry, P., Laxon, S., Mallow, U., Mavrocordatos, C., Phalippou, L., Ratier, G., Rey, L., Rostan, F., Viau, P., Wallis, D., 2006. Cryosat: a mission to determine the fluctuations in Earth's land and marine ice fields. *Adv. Space Res.* 37, 841–871.
- Wingham, D.J., Giles, K.A., Galin, N., Cullen, R., Armitage, T.W.K., Smith, W.H.F., 2018. A semianalytical model of the synthetic aperture, interferometric radar altimeter mean echo, and echo cross-product and its statistical fluctuations. *IEEE Trans. Geosci. Remote Sens.* 56, 2539–2553.